JOURNAL OF Applied Polymer SCIENCE

Effect of Drawing on the Molecular Orientation and Polymorphism of Melt-Spun Polyvinylidene Fluoride Fibers: Toward the Development of Piezoelectric Force Sensors

Kevin Magniez,[1] Andrew Krajewski,[2] Martin Neuenhofer,[3] Richard Helmer[2]

[1]Institute for Frontier Materials, Deakin University, Victoria, Australia

[2]Commonwealth Scientific and Industrial Research Organisation (CSIRO), Materials Science and Engineering division, Victoria, Australia

[3]Institut für Textiltechnik, RWTH Aachen University, Germany

Correspondence to: K. Magniez (E-mail: kmagn@deakin.edu.au)

ABSTRACT: Thin piezoelectric polyvinylidene fluoride fibers containing a high piezoelectric β-phase content of up to 80% were developed in this work using a melt-spinning process. After crystallization from the melt, the fibers were subsequently stretched unidirectionally at 120°C between 25 and 75% of their original length. The effects on the molecular orientation, polymorphism and tensile properties of the fibers were investigated. Polarized infra-red spectroscopy and X-ray diffraction results show that the conversion of α-phase to β-phase occurred during the stretching process as a result of molecular alignment and creation of a dipole induced by the CF_2 groups normal to the fiber direction. These fibers were then integrated into various weave architectures in order to design flexible two-dimensional textile-based piezoelectric force sensors. The piezoelectric responsiveness of these materials, tested under impact (70 Newton force, 1 Hz frequency) was very promising, with a maximum output voltage of up to 6 V and an average sensitivity of up to 55 mV/N measured. © 2013 Wiley Periodicals, Inc. J. Appl. Polym. Sci. 129: 2699–2706, 2013

KEYWORDS: textiles; sensors and actuators; structure-property relations

Received 22 October 2012; accepted 8 January 2013; published online 30 January 2013
DOI: 10.1002/app.39001

INTRODUCTION

The growing demand for new and exciting functionalities into textiles has been responsible for the scientific and industrial research efforts on smart clothing.[1] The inclusion of functional electro-active fibers into textiles has consequently been actively investigated over the past few years, potentially providing the textile industry with a new technological platform for sensing, health monitoring and energy harvesting applications.[2] Much of the previous reported work in this field has shown that ceramic-based piezoelectric devices perform better than their polymer-based counterparts[3,4]; however, the brittleness of ceramic materials has hindered their implementation in textile. As a result there has been a shift to exploring polymer-based piezoelectric technologies which offer more flexibility in design and processing. The main scientific challenge remains in developing a functional piezoelectric polymeric fiber which can be easily meshed into a hybrid textile structure. Only a handful of scientific studies have been published to date on the use of piezoelectric polymer based fibers for smart textiles.[2,5–7]

Out of the many synthetic polymers which have demonstrated piezoelectric properties; polyvinylidene fluoride (PVDF) has shown useful piezoelectric properties. PVDF is the principal commercially available piezoelectric polymer, typically produced in the form of films of thickness varying from 10 to 800 μm.[8] PVDF is a semicrystalline polymer presenting pronounced polymorphic crystalline forms.[9,10] The most studied and important polymorphs are α- and β-phases, with most of the scientific focus being on improving or optimizing the β crystal phase content in PVDF as it is the component responsible for the piezoelectrical properties. The evolution of the piezo β phase content during the processing of films or fibers has been addressed in several papers, showing some correlation with the stretching ratios and temperatures.[11–15] Siores et al.[16] recently described a continuous melt-spinning process for the development of piezoelectric PVDF fibers using a corona discharge, showing that the piezoelectric properties of the fibers can be optimized by controlling the cold drawing temperature, drawing ratio and applied electric field.

Additional Supporting Information may be found in the online version of this article.

The combination of flexible piezoelectric fibers with conventional fibers and conductive electrodes into a textile weave has been described as an ideal way to make wearable piezoelectric clothing.[17] This is because in woven structures, the piezoelectric fibers (acting as charge generator) can interconnect with the conductive electrodes in a number of ways; however, the choice of both design and conductive charge carrier has to be carefully considered for optimum performance. Moreover, the surface area offered by piezoelectric fibers is greater than that offered by film and therefore one would expect an improvement in piezoelectric performance when using piezoelectric fibers rather than a film in piezoelectric clothing. The objective of this research was to develop a woven-based piezoelectric sensor and the approach involved two stages. In the first stage, we produced a range of melt-spun piezoelectric PVDF fibers and we analyzed the effect of processing on the structure property relationships and the development of the piezo electric crystal phase. In the second stage, we integrated these fibers into various weave architectures to explore the design and optimization of two-dimensional (2D) textile-based piezoelectric force sensors. The effectiveness of the sensors was tested under impact. The practicability of the piezoelectric textile devices is discussed for certain application environments.

MATERIALS AND EXPERIMENTAL METHODS

Materials

PVDF Kynar 710 was sourced from Arkema. Kynar 710 is a low molecular weight PVDF having a number average molecular weight (M_n) in the range of 70,000 to 80,000 g/mol. The polymer melts between 165 and 170°C and has a density of approximately 1.78 g/cm^3.

Melt-Spinning of the Fibers

PVDF was converted into homogenous fibers using a Busschaert bicomponent extruder (35-mm screw diameter, length to diameter ratio of 30 : 1). The spinneret constituting the bottom distribution plate on the spinning pack contained 20 holes each of 0.5-mm diameter. The volume of PVDF flowing through the spinneret was controlled and it varied between 50 and 100 cm^3/min. The temperature profile on the extruder ranged from 260 to 280°C. After quenching, the multifilament bundle of PVDF passed through the godet roller system consisting of several cold and heated rolls in the following sequence: melt-drawing roll (R_1), two cold rolls (R_2), two induction heated rolls (R_3), and finally two cold rolls (R_4) as previously described.[18] The fibers coming off the final roll were then wound onto a bobbin. The fibers were drawn to 25, 50, and 75% of their original length by adjusting the speeds of the cold and heated rolls (Table I). The temperature of the heated rolls varied between 105 and 120°C. The degree of melt drawing was fixed by setting the velocity of the first roll R_1 at 500 m/min.

Characterizations and Measurement

Tensile Properties. The PVDF fibers were conditioned for 24 h prior to testing and the testing was carried out in a controlled environment at 20 ± 2°C with 65 ± 2% relative humidity according to ISO 139:2005 standard. Tensile tests were performed in accordance with the ASTM method D3822-96 (Standard Test Method for Tensile Properties of Single Textile Fibres) using a SIFAN 2 (BSC Electronics) single fiber tensile tester. An extension of 500 mm/min over an effective gauge length of 200 mm with a pretension of 0.5cN/tex was used. At least 20 single fibers were measured for each batch. The modulus, tenacity and elongation at break of the fibers were determined.

Table I. Cold Drawing Parameters During Melt-Spinning

	Velocity (m/min)/Temperature (°C) at % draw ratio		
Roll	25	50	75
R_1	500/RT	500/RT	500/RT
R_2	625/105	725/105	750/105
R_3	625/120	750/120	900/120
R_4	625/RT	750/RT	900/RT
Winder	600/RT	750/RT	900/RT

RT: Room temperature (20°C ± 2°C).

X ray Analysis. The PVDF fibers were wound unidirectionally onto a single crystal Silicon substrate (zero background). The fibers were scanned perpendicular to the axis direction using a PANalytical X-ray spectrometer (Copper X-ray source, λ = 1.5418 Å), between 10 and 40° of 2θ with a 0.02° step (with a 2 s scan time).

Fourier Transform Infrared Spectroscopy (FTIR). Infrared data were collected on a Bruker Vertex 70 FTIR equipped with an attenuated total reflectance (ATR) unit using a bundle of PVDF fibers. The spectra (64 scans at 4 cm^{-1} resolution) between 600 and 1600 cm^{-1} were obtained in ATR mode.

Molecular Orientation Using Optical Birefringence. A single filament was placed on a microscope slide between crossed polarizers in an Olympus BX50 optical microscope equipped with a full-wave retardation plate. The optical birefringence of the fibers was measured by rotating to a position of maximum brightness (+45°/−45°) to visualize the polarization color referred to as interference color resulting from the retardation between the ordinary and extraordinary waves.[18] Quantitative analysis of the interference colors observed was accomplished by consulting a Michel–Levy chart. The full retardation plate was used to shift the interference color of one full wave (±530 nm) to determine the order of polarization colors (which was of first, second, or third order generally).

Production and Evaluation of Piezoelectric Force Sensors. A series of woven fabrics were constructed using the melt-spun PVDF multifilament yarn produced at a flow rate of 80 cm^3/min with a draw ratio of 75%. In this work, we demonstrated their potential use as piezoelectric sensors using an integrated 2D design. The PVDF fibers and conductive fibrous electrodes were integrated into a plain polyester weave and a 2/2 twill weave to produce a 2D flexible piezoelectric woven sensor (Figure 1). The woven structure contains nonconductive nylon yarn spacer, separating the conductive yarn from one another to avoid shortening. The warp in the sensing area consists of

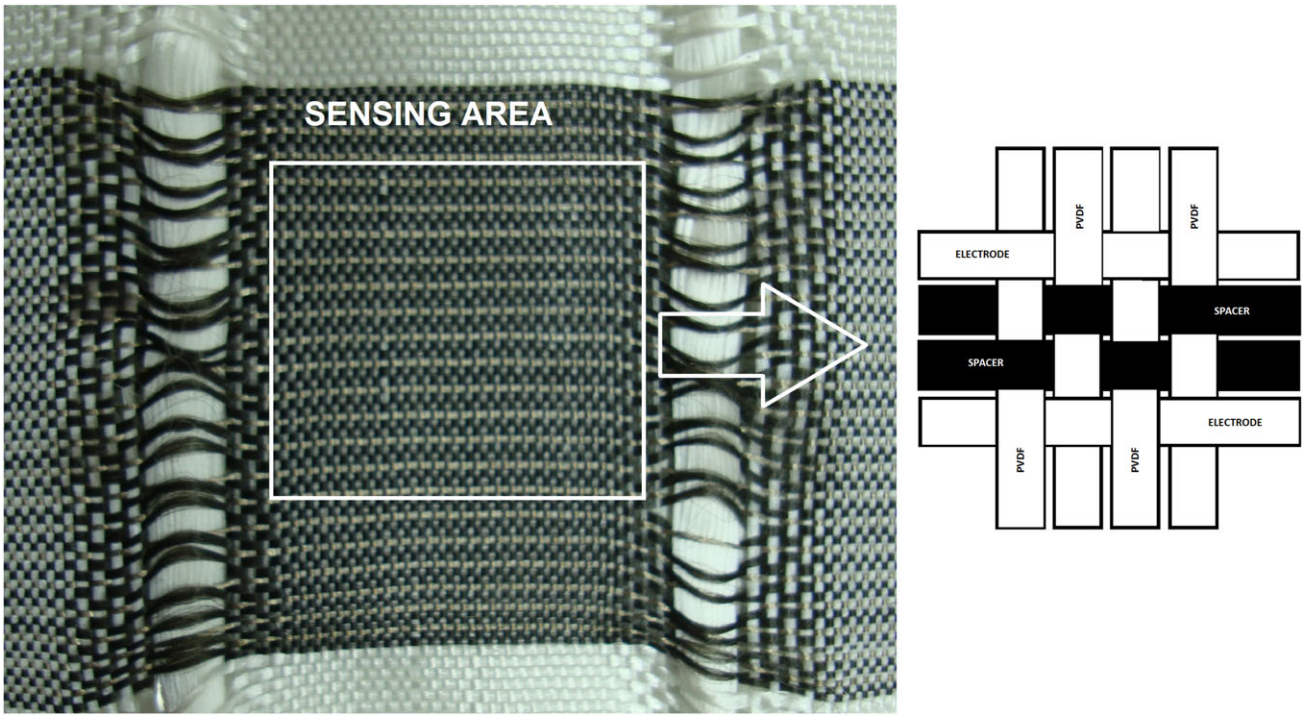

Figure 1. Configuration of the 2D flexible piezoelectric woven sensor. The sensing area is highlighted in the middle. The polyester and PVDF yarns are white; the nylon spacer yarns are black. The weave structure in that area is highlighted on the right hand side. [Color figure can be viewed in the online issue, which is available at wileyonlinelibrary.com.]

PVDF yarn, outside the sensing area it consists exclusively of polyester yarn. The weft consists of polyester outside the sensing area and inside the sensing area it consists of conductive yarn (silver-coated nylon) and nonconductive spacer yarn (nylon). Every second conductive yarn is connected to form the two electrodes. The conductive fibrous electrodes were connected to a copper strip using conductive epoxy glue. Each electrode was connected to a metallic pushbutton via insulated electrical wire. The pushbutton performed as a physical connector between the sensor and the measuring instrument.

The responsiveness of the flexible textile PVDF sensors was tested under impact. The frequency of the impact was 1 Hz and the force generated during impact was approximately 70 Newton. To prevent the samples from moving, they were fixed on a wooden plate on which a very thin foam film (2 mm) was glued in order to reduce the noise of the impact and to prevent damage to the sensor. The tip of the impact tester consists of two parts and the load cell (Figure 2). The upper part is fixed to the piston and the load cell is fixed underneath it with a certain clearance and secured by screws. The lower part is fixed with a screw to the load cell. In this configuration, the force between the two parts is transmitted directly to the load cell during impact. The load cell and the electrodes of the sensor were connected to a computer to record the data.

RESULTS AND DISCUSSION

During the drawing process, the filaments were heated up above the glass transition of the polymer and were stretched several times their length. The effect of draw ratio on the tensile properties of single PVDF filaments is illustrated in Figure 3. This process induced alignment of the polymer chains[18] which in turn increased the Young's modulus and tenacity of the

Figure 2. The tip of the impact tester consisting of two parts and the load cell. [Color figure can be viewed in the online issue, which is available at wileyonlinelibrary.com.]

Applied Polymer SCIENCE

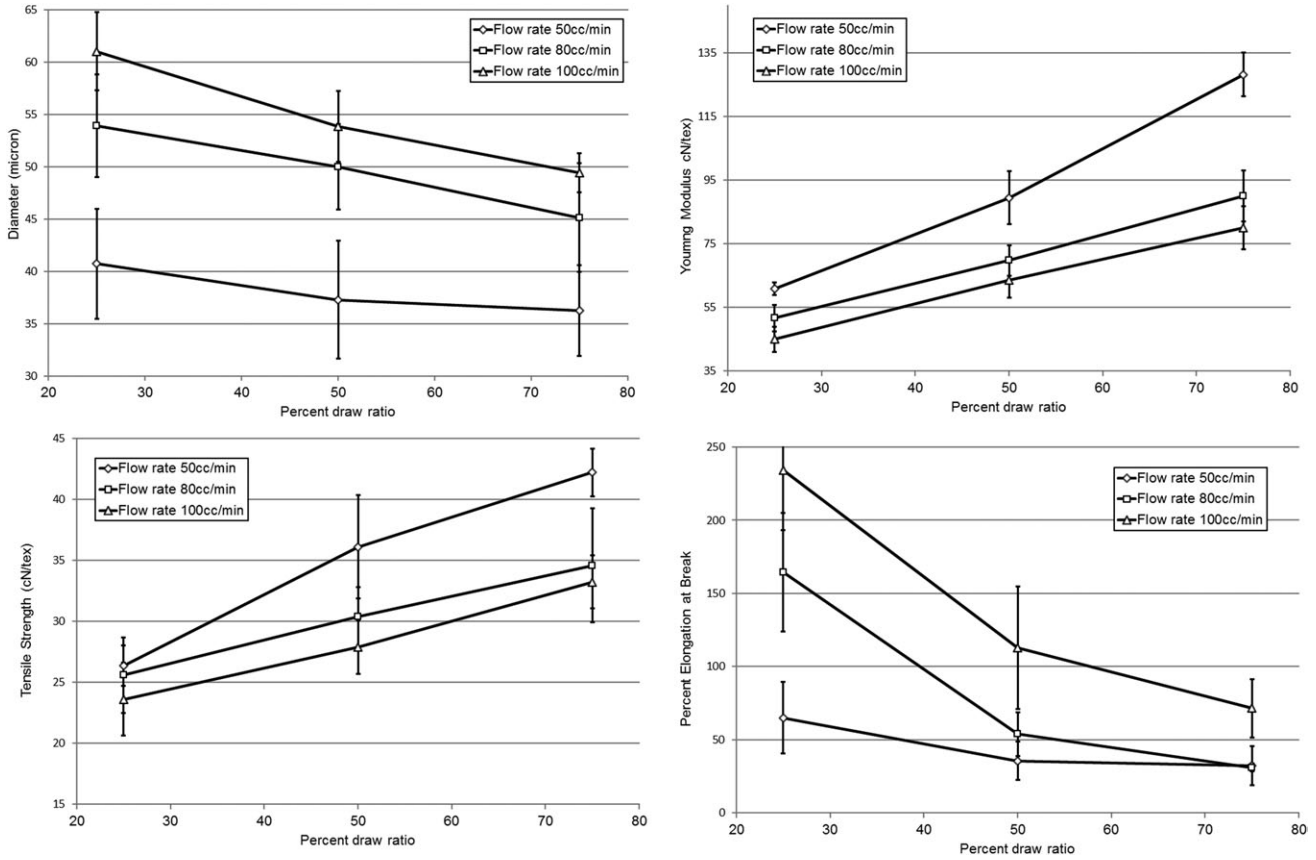

Figure 3. Tensile results on single PVDF filaments.

filaments by up to 110 and 60%, respectively. A decrease in the stretchability of the filaments was noted however it is still at its very worst 30%. After an extensive drawing of 75%, fine PVDF filaments were produced with diameter comprised between 36 and 50 μm, and tensile strength between 33 and 43 cN per tex, all well within the range of values found in commercial synthetic fibers.[19] This is also very comparable to the thickness of metallized piezoelectric PVDF commercial films (i.e., 30 and 50 μm).[20] It was also noted that the crystallinity of the PVDF increased steadily during the stretching process; reaching up to 47% comparable to Du et al.[21] who reported the effect of stretching on the crystalline phase structure of melt-spun PVDF fibers (see Supporting Information Figure S1 and S2).

The changes in molecular orientation exhibited by the PVDF fibers were evaluated by measuring the birefringence of the fibers from their polarization color. It can be seen from Figure 4 that the birefringence increased linearly upon drawing, thus reflecting alignment and orientation of the chains. A maximum birefringence value of approximately 0.043 was observed, which is comparable to the values reported by Cakmak and Wang[11] in PVDF films and fibers.

The mechanism of solid phase transformation of the monoclinic α form into the orthorhombic β piezo form during stretching of PVDF has been reported elsewhere.[10,15] A clear indication of a change in polymorphic behavior of the PVDF fibers is discernible in the corresponding X-ray diffraction patterns (Figure 5). Upon drawing, the (100), (020), (021), and (002) reflection peaks at 17.7°, 18.4°, 19.9°, 26.6°, and 33° of 2θ, corresponding to the α-crystal phase is attenuated, whilst the reflection peak of the β-crystal phase at 20.3° and 36° of 2θ become more intense (110, 200, and 001).[10,14,22]

FT-IR spectroscopy was utilized to easily quantify the relative phase content of the most common α and β polymorphic crystal forms (Figure 6). The absorption bands at 615, 765, 800, 980, and 1075 cm^{-1} are characteristic of the α crystal phase, whilst the β crystal phase appears at 840 and 1276 cm^{-1}.[13,23]

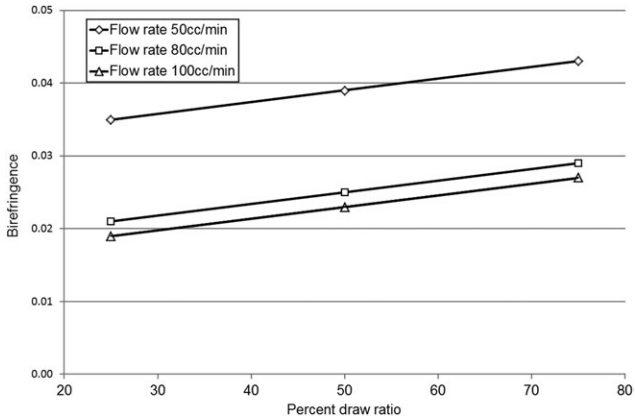

Figure 4. Optical Birefringence of the cold-drawn PVDF fibers.

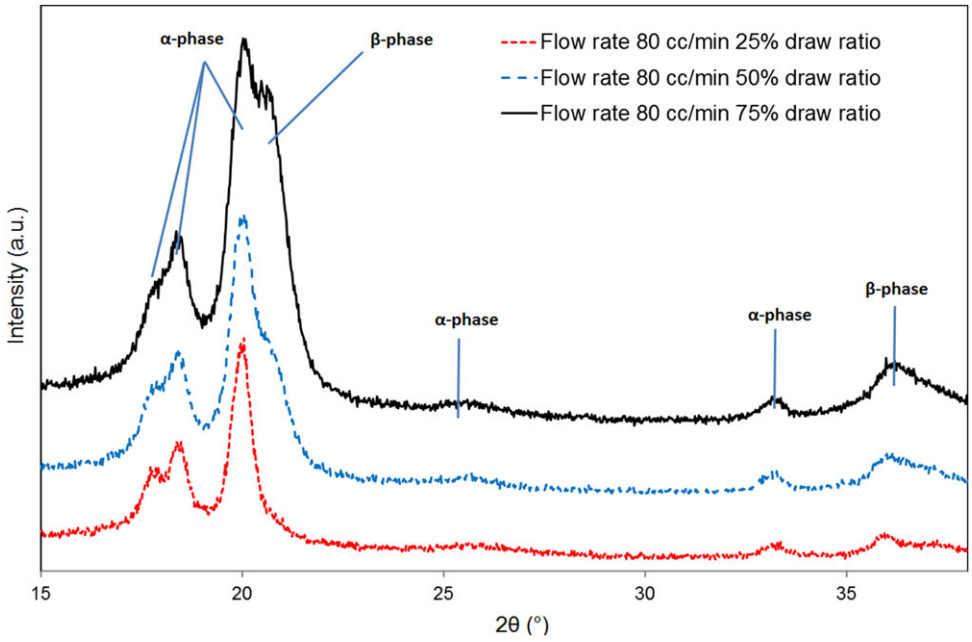

Figure 5. X-ray diffraction patterns of the PVDF fibers processed at 80 cm^3/min and drawn 25, 50, and 75% of their original length (only shown here for brevity). The data has been shifted vertically for clarity. [Color figure can be viewed in the online issue, which is available at wileyonlinelibrary.com.]

The fraction of β phase present can be calculated using the procedure explained by Gregorio and Cestari.[9] The relative fraction $F(\beta)$ of the β phase can then be calculated using:

$$F(\beta) = \frac{\chi_\beta}{\chi_\alpha + \chi_\beta} = \frac{A_\alpha}{1.26A_\alpha + A_\beta}$$

where χ_α and χ_β are the degrees of crystallinity of each phases, and A_α and A_β correspond to absorption bands for α and β phases, respectively. The absorption bands at both 766 and 840 cm^{-1} were selected for the α and β phase, respectively. We found that this method is quite reliable and the results correlate well with deconvolution data of the XRD diffractograms (see Supporting Information Figure S3).

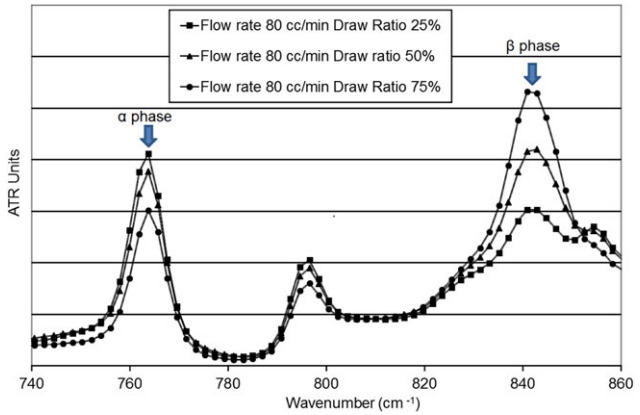

Figure 6. FT-IR spectra showing the changes in the absorbance A_α and A_β for PVDF fibers produced at a flow rate of 80 cm^3/min and cold drawn between 25 and 75% of their initial length. [Color figure can be viewed in the online issue, which is available at wileyonlinelibrary.com.]

It was found that at the lowest drawing ratio of 25%, the β phase content was the highest for the sample produced at 50 cm^3/min (Figure 7). This is explained by the fact that the β phase content is predominantly stress-induced from the melt[24] and the filaments produced at the lowest flow rate would have been under higher melt-stresses at the spinning holes. At a drawing ratio of 75%, a maximum β phase content of 80% was obtained. When the flow of polymer is increased at the melt spinning head, the thickness of the fiber is increased which consequently decreases the β phase content. Nonetheless, after an extensive drawing of 75%, the β phase content reached 50–60% at flow rates of 80 and 100 cm^3/min.

FTIR analysis using polarized light in perpendicular ($\perp$) and parallel ($\parallel$) modes also showed that the intensity of the CF_2 bending and stretching vibration assigned to the α and β crystal phases[12,23] are much weaker when the light is polarized

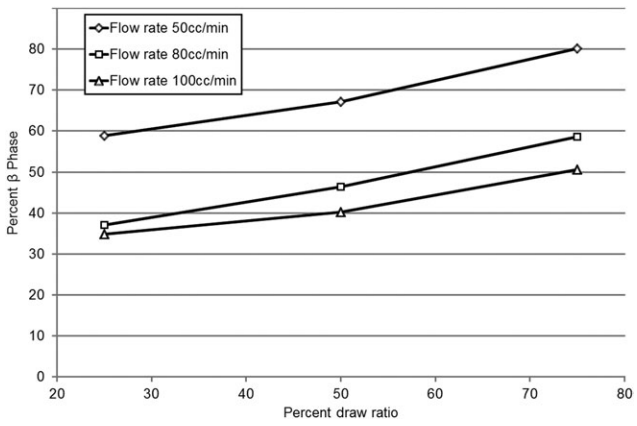

Figure 7. Evolution of the β piezo crystal content (bottom) in PVDF fibers upon cold drawing.

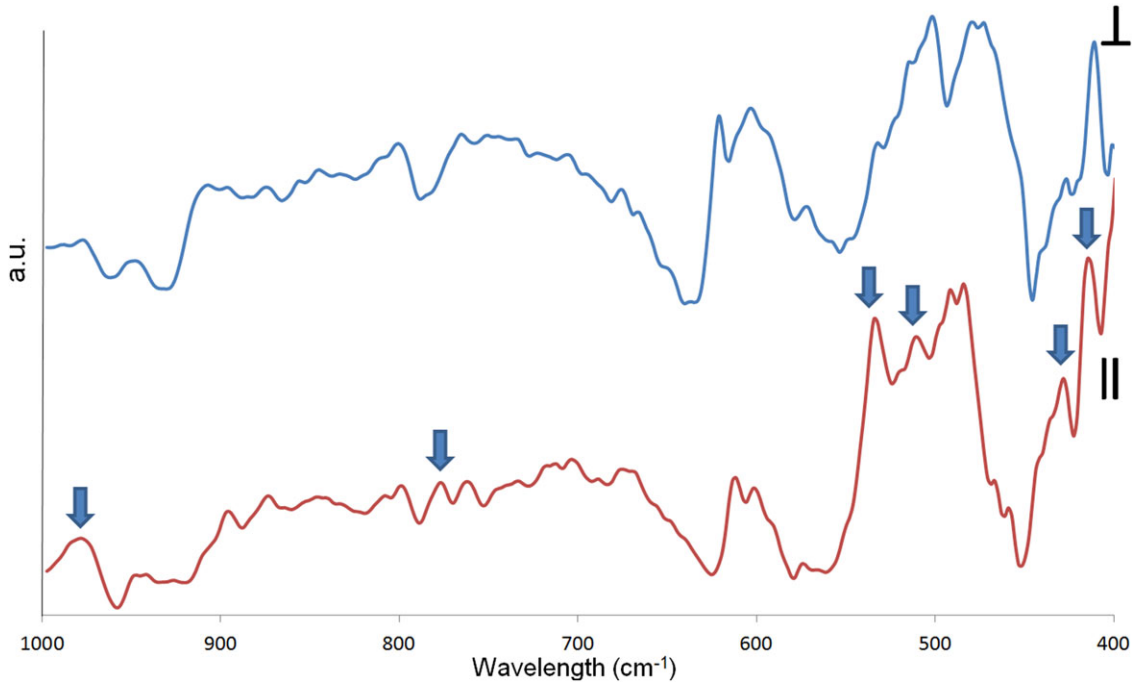

Figure 8. Perpendicular (⊥) and parallel (||) polarized FT-IR spectrum (data shifted vertically for clarity) in transmission mode for PVDF fibers produced at a flow rate of 80 cm^3/min and cold drawn at 75% of their initial length. The arrows highlight α and β crystal phase absorption peaks. The data has been shifted vertically for clarity. [Color figure can be viewed in the online issue, which is available at wileyonlinelibrary.com.]

perpendicular to the fiber axis, indicating that the polymer chains are preferentially orientated along the fiber axis (Figure 8). This strongly suggest the creation of a dipole induced by the CF_2 groups normal to the fiber direction during drawing as reported elsewhere in films.[15,25]

Integration of the PVDF Fibers into Piezoelectric Sensors

The PVDF fibers were introduced into a flexible weave textile and we then demonstrated the potential of these materials as 2D piezoelectric force sensors. During the weaving process however, the fibers are exposed to mechanical friction, which can lead to imperfection and breakages if the filaments are mechanically too weak. Although the filaments processed at a flow rate of 50 cm^3/min with 75% draw ratio had the highest piezo β-phase content (approximately 80%), these were too thin (36 μm^3) and fragile and thus difficult to weave into fabric. As a result, we used the PVDF fibers processed at a flow rate of 80 cm^3/min with a 75% draw ratio (β-phase content of approximately 60%) to prepare the piezoelectric force sensors. The handling of the 45 μm PVDF fibers produced under these conditions was easier and it led to fewer fiber breakages.

The output voltage measured on the 2D sensors upon a 1 Hz frequency, 70 Newton spike-shaped stimulus (Figure 9) was found to reach up to 6 V at maximum, with an average of 3–4 V (Figure 10). By comparison, Ichiki et al.[26] studied the piezoelectric behavior of a zirconate titanate disk under 40 Newton impact load, reporting an output voltage of 1.8 V. Guillot et al.[27] integrated both piezoelectric PVDF films into a fabric as a basis for the construction of systems capable of harvesting mechanical energy from the environment, reporting an electrical response of 200 mV (under vibration at 4.6 Hz). Fang et al.[28] used a complex electrospinning process to produce nano-size PVDF fibrous webs. At 1 Hz compression impact, the nano-fibrous matts displayed a 0.43 V output, and by increasing the frequency to 10 Hz, the author obtained values similar to ours. Jiang et al.[29] very recently described a cardiorespiratory sensor using PVDF films and a flexible PDMS substrate for human health monitoring application. Cardiorespiratory detection results in bending mode showed an output voltage of up to 5 V. The fabrication process is however quite complex (as the substrates needs to be patterned and the PVDF film is deposited using an ionized evaporation technique).

Piezoelectric sensors do not have a minimum voltage output requirement however; their ability to detect the type and magnitude of the stimulus is only limited by the sensitivity of the measuring interface.[5] Commercially, the sensitivity of impact sensors (quartz based) is of approximately 10–20 mV/N[30] but can reach up to 125 mV/N.[31] The sensitivity of the sensors designed in this article (up to 55 mV/N, Figure 10) is in fact very good in comparison to what is commercially available. Wang et al.[32] reported values of up to 42 mV/N using electrospun PVDF nanofibers which again is much more difficult to produce practically.

CONCLUSIONS

In this work, melt-spun PVDF fibers containing a high piezoelectric β- phase content of up to 80% were developed by melt-spinning and without the need for corona discharge. This was achieved through careful optimization of the processing parameters such as polymer flow rates and drawing ratios, allowing for optimum alignment of the polymer chains and conversion of the α crystal phase to the β piezoelectric crystal phase. These fibers were

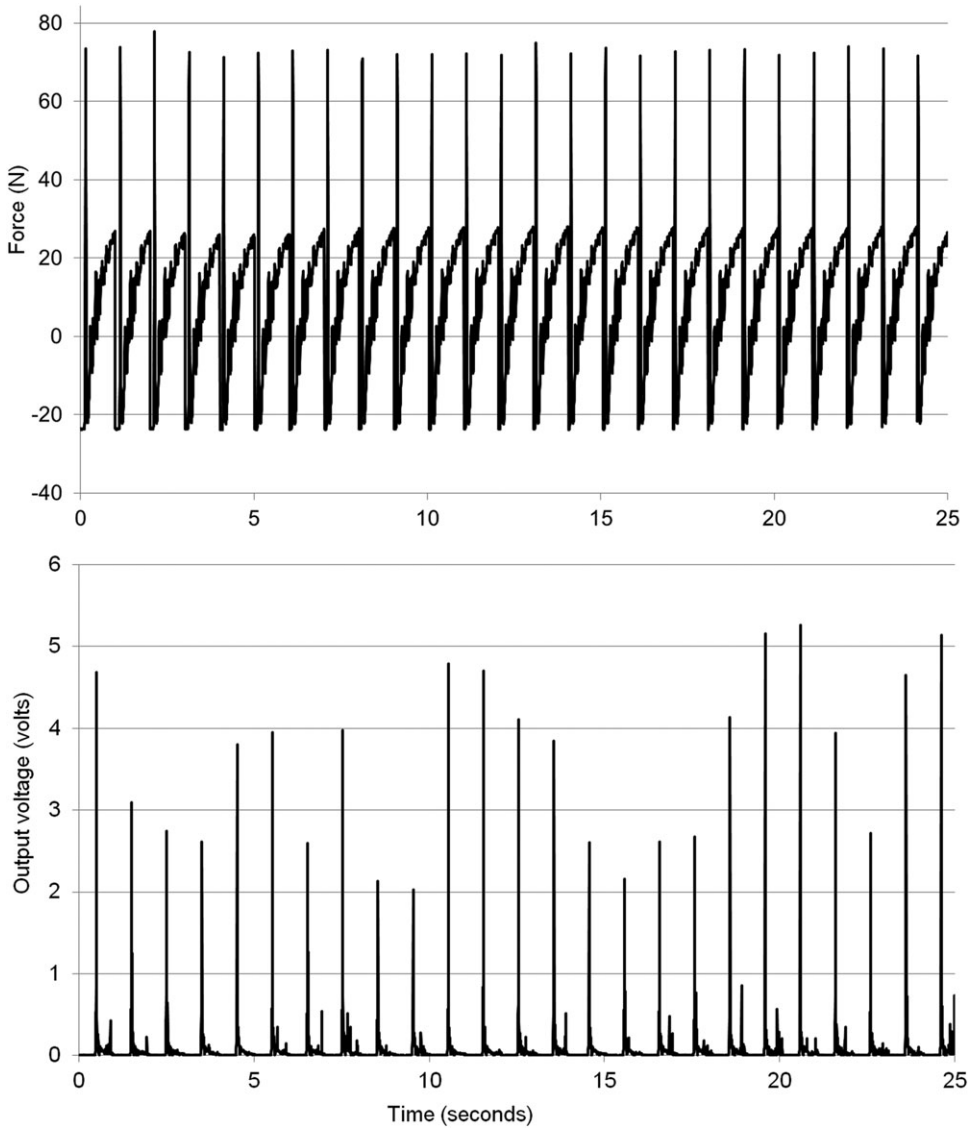

Figure 9. Output voltage measured on the 2D sensors upon a 1 Hz frequency, 70 Newton spike-shaped stimulus (bottom curve).

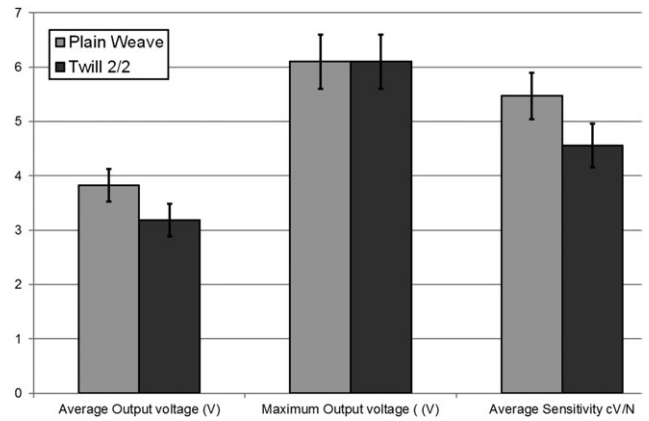

Figure 10. Piezoelectric performance under impact of on the 2D plain weave sensors (note that the sensitivity is displayed in cN/V for visual clarity).

subsequently integrated into various weave architectures to design flexible wearable 2D textile-based piezoelectric force sensors. The outcomes of this study showed that the performance of these sensors under impact were comparable to other commercially available ceramic based sensors. This case study demonstrated a valid approach to a wearable textile based smart sensor and also highlighted the unique attribute and advantages of piezoelectric textiles.

ACKNOWLEDGMENTS

The authors gratefully acknowledge the financial support of CSIRO Materials Science and Engineering, the weaving and workshop staff without whom, this work would be just another idea.

REFERENCES

1. Lymberis, A.; Paradiso R. In Smart fabrics and interactive textile enabling wearable personal applications: R&D state of the art and future challenges, Proceedings of the 30th

Annual International Conference of the IEEE on Engineering in Medicine and Biology Society, Vancouver, Canada, August 20–25, **2008**; p 5270.

2. Huang, C. T.; Sheng, C. L.; Tang C. F.; Chang S. H. *Sens. Actuators A* **2008**, *141*, 396.
3. Patel, I.; Siores, E.; Shah, T. *Sens. Actuators A* **2010**, *159*, 213.
4. Swallow, L. M.; Luo, J. K.; Siores, E.; Patel, I.; Dodds, D. *Smart Mater. Struct.* **2008**, *17*, 025017.
5. Edmison, J.; Jones, M.; Nakad, Z.; Martin, T. In Using piezoelectric materials for wearable electronic textiles, Proceedings of the 6th International Symposium on Wearable Computers, Washington, USA, October 7–10, **2002**; p 41.
6. Jeong, J. W.; Jang, Y. W.; Lee, I.; Shin, S.; Kim, S. In Wearable Respiratory Rate Monitoring using Piezo-resistive Fabric Sensor, IFMBE Proceedings of the World Congress on Medical Physics and Biomedical Engineering. Munich, Germany, September 7–12, **2009**; p 282.
7. Huang, C. T.; Tang, C. F.; Lee, C. M.; Chang, S. H. *Sens Actuators A* **2008**, *148*, 10.
8. Vinogradov, A. M.; Hugo, S. V.; Tuthill, G. F.; Bohannan, G. W. *Mech. Mater.* **2004**, *36*, 1007.
9. Gregorio, J. R.; Cestari, M. *J. Polym. Sci. Part B: Polym. Phys.* **1994**, *32*, 859.
10. Gregorio, R.; Ueno, E. M. *J. Mater. Sci.* **1999**, *34*, 4489.
11. Cakmak, M.; Wang, Y. *J. Appl. Polym. Sci.* **1989** *37*, 977.
12. Lanceros-Méndez, S.; Mano, J. F.; Costa, A. M.; Schmidt, V. H. *J. Macromol. Sci. Part B* **2001**, *40*, 517.
13. Salimi, A.; Yousefi, A. A. *Polym. Test.* **2003**, *22*, 699.
14. Satapathy, S.; Pawar, S.; Gupta, P.; Varma, K. *Bull. Mater. Sci.* **2011** *34*, 727.
15. Sencadas, V.; Gregorio, R.; Lanceros-Méndez, S. *J. Macromol. Sci. Part B* **2009** *48*, 514.
16. Siores, E.; Hadimani, R. L.; Vatansever, D. (Universoty of Bolton). US Patent WO/2012/035350, April **2012**.
17. Vatansever, D.; Siores, E.; Hadimani, R. L.; Shah, T. In Advances in Modern Woven Fabrics Technology, 1st ed.; Vassiliadis, S., Ed.; InTech Europe, **2011**; p 23.
18. Magniez, K.; Fox, B. L.; Looney, M. G. *Polym. Compos.* **2011**, *32*, 604.
19. Bunsell, A. In Handbook of Tensile Properties of Textile and Technical Fibres; Bunsell, A. R., Ed.; Woodhead Publishing: Manchester, England, **2009**.
20. Measurement Specialties Inc., Available at: www.msiusa.-com (accessed October 2012).
21. Du, C. H.; Zhu, B. K.; Xu, Y. Y. *J. Appl. Polym. Sci.* **2007**, *104*, 2254.
22. Zhao, X.; Cheng, J.; Chen, S.; Zhang, J.; Wang, X. *J. Polym. Sci. Part B: Polym. Phys.* **2010** *48*, 575.
23. Bormashenko, Y.; Pogreb, R.; Stanevsky, O.; Bormashenko, E. *Polym. Test.* **2004**, *23*, 791.
24. Wang, Y.; Cakmak, M.; White, J. L. *J. Appl. Polym. Sci.* **1985**, *30*, 2615.
25. Gasmi, A.; Lewa, C.; Łętowski, S. *Mater. Lett.* **1992** *13*, 346.
26. Ichiki, M.; Ashida, K.; Kitahara, T. *Jpn. J. Appl. Phys. Part 1* **2002**, *41*, 7080.
27. Guillot, F. M.; Beckham, H. W.; Leisen, J. *J. Acoust. Soc. Am. 128*, 2340.
28. Fang, J.; Wang, X.; Lin, T. *J. Mater. Chem.* **2011**, *21*, 11088.
29. Jiang, Y.; Hiroyuki, H.; Syohei, S.; Kensuke, K.; Takayuki, F.; KoheI, H.; Kazusuke, M. *Procedia Eng.* **2010**, *5*, 1466.
30. PCB Piezoelectronics, Available at: http://www.pcb.com (accessed October 2012).
31. Fuji Ceramics Corporation, Available at: http://www.fujicera.co.jp (accessed October 2012).
32. Wang, Y. R.; Zheng, J. M.; Ren, G. Y.; Zhang, P. H.; Xu, C. *Smart Mater. Struct.* **2011**, *20*, 045009.